



## New insights into the accessibility of native cellulose to environmental contaminants toward tritium behavior prediction

A.-L. Nivesse<sup>a,b</sup>, N. Baglan<sup>c</sup>, G. Montavon<sup>a</sup>, O. Péron<sup>a,\*</sup>

<sup>a</sup> Subatech, UMR 6457, 4, rue Alfred Kastler, BP 20722, 44307 Nantes Cedex 3, France

<sup>b</sup> CEA, DAM, DIF, F-91297 Arpajon, France

<sup>c</sup> CEA, DIF, DRF, JACOB, IRCM, SREIT, LRT, F-91297 Arpajon, France

### ARTICLE INFO

Editor: Dr. L. Angela Yu-Chen

#### Keywords:

Tritium  
Speciation  
Isotopic exchange  
Cellulose  
Pollutants

### ABSTRACT

Tritium speciation and behavior in the environment directly rely on accessible OH groups of organic molecules and their hydrogen exchangeability properties. As one of the most widespread biomolecule, cellulose role in reducing the exchange capacity of the hydrogen atom has been previously highlighted experimentally in various environmental matrices. In this paper, a robust and reliable T/H gas-solid isotopic exchange procedure has been implemented to assess the OH group accessibility of native celluloses with an increasing degree of crystallinity. A linear relationship was found between hydroxyl reactivity and the crystallinity index (CrI) of native celluloses, as determined by the analysis of their crystalline structure from XRD characterization. The application of the obtained linear experimental model to cellulosic materials was then evaluated and an acceptable minimum value of 12% for the CrI parameter on environmental matrices could thus be established. The authors have therefore proposed an environmental matrices relevant and efficient analytical process in order to determine the accessibility of native cellulose hydroxyl groups to tritium in the environment from a single and quick sample characterization procedure.

### 1. Introduction

Tritium is the natural radioactive isotope of hydrogen and one of the main radionuclides released into the environment by nuclear installations (IRSN, 2017). According to current forecasts, the release rates of this radionuclide are expected to rise significantly over the upcoming decades from changes in fuel management methods along with new tritium-emitting facilities, such as the International Thermonuclear Experimental Reactor (ITER) and Evolutionary Power Reactor (EPR) (ASN, 2010; Song et al., 2019). To understand the behavior of this radioactive pollutant in the environment and thus evaluate its potential impact, the main scientific challenge calls for identifying its mobility and bioavailability characteristics, which are mainly governed by its speciation. In environmental matrices, tritium can integrate organic matter in the form of organically bound tritium (OBT) by replacing stable hydrogen isotopes and taking up exchangeable positions (exchangeable OBT) or else remaining in the molecule until its degradation (non-exchangeable OBT) (Diabaté and Strack, 1993; Kim et al., 2013; Sepall and Mason, 1961). As such, monitoring OBT has become a major concern in many countries for both public and regulatory

assurance and several studies have focused on the non-exchangeable form (NE-OBT) as a reliable environmental marker (Kim et al., 2013; Péron et al., 2016; Baglan et al., 2018; Nivesse et al., 2021a, 2021b). Among those previous investigations, cellulose has been repeatedly identified as one of the organic molecule with great impact on OBT speciation and was found to be responsible for the decrease in tritium exchangeability rates within various cellulosic environmental matrices (Nivesse et al., 2021a; Péron et al., 2018). Beyond these properties specific to the cellulose biomolecule, the work presented in Nivesse et al. (2021a) has also highlighted the total control of major constituent over the hydrogen transfer mechanisms and OBT speciation found in related environmental matrices. As the most abundant biopolymer on earth and the main structural component of cell walls in plants, cellulose reactivity to hydrogen isotopes binding is thus key to understanding tritium behavior in the environment and its transfer into food chain samples.

In cellulose molecules, OBT speciation directly relies on accessible OH groups and their hydrogen exchangeability properties. On the supramolecular level, cellulose is composed of linear chains of D-glucose units linked together by (1→4)-beta-D-glycosidic bonds, subjected to aggregation into microfibrils with a sheet organization and a two-phase

\* Corresponding author.

E-mail address: [olivier.peron@subatech.in2p3.fr](mailto:olivier.peron@subatech.in2p3.fr) (O. Péron).

<https://doi.org/10.1016/j.jhazmat.2021.126619>

Received 14 April 2021; Received in revised form 14 June 2021; Accepted 8 July 2021

Available online 11 July 2021

0304-3894/© 2021 Elsevier B.V. All rights reserved.

morphology of crystalline and amorphous regions. The crystalline structure of cellulose is highly ordered and originates from extensive intra-molecular and intra-strand hydrogen bonding between OH groups. As a result, the accessibility of cellulose hydroxyl groups undergoes a drastic reduction, as has been widely demonstrated in the literature during crystalline structure investigations of various cellulose compounds in hydrogen-deuterium exchange experiments (Lindh and Salmén, 2017; Reishofer and Spirk, 2015). Nevertheless, no clear analytical relationship has ever been derived between hydrogen exchangeability and degree of crystallinity in native cellulose. To a global extent, several characterizations methods (SEM, TEM, FTIR, XRD, TGA ...) are usually combined to assess the link between the crystalline morphology of cellulose and applications related to its OH group's reactivity (Luzi et al., 2019; Melikoğlu et al., 2019; Trache et al., 2016). However, simplified calculation method could also be fit for purpose in given conditions. For example, the crystallinity index (CrI) determined after a single X-ray diffraction (XRD) analysis is commonly used for quantifying the crystallinity rate of native cellulose (Hashem et al., 2020; Johar et al., 2012; Luzi et al., 2019; Madivoli et al., 2016; Melikoğlu et al., 2019; Segal et al., 1959; Trache et al., 2016). The present work therefore aims to provide a simple and environmental matrices relevant linear model to describe OH group accessibility with respect to the crystallinity index (CrI) from a series of five native celluloses. While CrI is determined by means of X-ray diffraction (XRD), OH group accessibility is investigated by a robust and reliable T/H gas-solid isotopic exchange procedure (Nivesse et al., 2021a, 2021b, 2020; Péron et al., 2018). By virtue of being extracted or investigated from environmental sources, the application potential of the linear model obtained for the cellulose accessibility determination can then be established for cellulosic materials and from direct measurements conducted on environmental matrices.

## 2. Materials and methods

### 2.1. Sample preparation and characterization

Alpha (cellulose-C) and microcrystalline (cellulose-E) native celluloses extracted from cotton sources (CAS number: 9004-34-6) were purchased from Sigma-Aldrich. The crystalline structures of these celluloses were modified by partial destruction using ball-milling processes. A series of five native celluloses with increasing crystalline ratios was produced from ball-milling with the following parameters: cellulose-A (142 x g, 15 min) and B (84 x g, 10 min) from cellulose-C (alpha cellulose); and cellulose-D (68 x g, 3 min) from cellulose-E (microcrystalline cellulose). Cellulose-E refers to the microcrystalline cellulose previously studied in Péron et al. (2018).

An amorphous compound of silica SiO<sub>2</sub> (CAS number: 7631-86-9) was purchased from Sigma-Aldrich and added in different ratios to each cellulose of the series (A through E) in order to obtain a modified sequence of increasing cellulose content samples (from 5% to 95% by weight) for each native cellulose of the series (Table 1).

All the samples were directly freeze-dried after the preparation steps and stored under vacuum prior to further use.

### 2.2. Experimental procedure

#### 2.2.1. X-ray diffraction analysis

X-ray diffraction was employed to determine the crystallinity of the series of five native celluloses and the modified sequences of increasing cellulose content samples. Each milled powder material was placed on the sample holder and leveled to obtain total and uniform X-ray exposure. Analyses were performed at room temperature using a D5000 Bruker X-ray diffractometer (Cu/K $\alpha$  radiation = 0.154 nm at 40 kV and 30 mA). The XRD patterns were collected within the range of  $2\theta = 0-50^\circ$  with a scan step of  $2\theta = 0.02^\circ$  and a measurement time per step of 4 s.

The crystallinity index (CrI) was determined based on the reflected intensity data, according to the method developed by Segal et al. (1959),

**Table 1**

Results on modified sequences of increasing cellulose content samples from celluloses A through E, along with their respective native cellulose ratio (% by weight), obtained sample CrI (%) and the resulting calculated native cellulose CrI (%) compared to the actual native cellulose CrI (%).

Native cellulose sequence	Sample	Native cellulose ratio (in % by weight)	Sample CrI (%)	Calculated native cellulose CrI (%)	Actual native cellulose CrI (%)
Cellulose A	A-1	60,3	–	–	13
	A-2	70,2	–	–	
	A-3	80,0	4	5	
	A-4	90,4	8	10	
	A-5	94,8	12	13	
Cellulose B	B-1	20,2	4	18	34
	B-2	30,0	9	30	
	B-3	35,6	12	34	
	B-4	40,1	14	34	
	B-5	50,1	17	34	
Cellulose C	C-1	15,5	4	26	46
	C-2	20,3	8	40	
	C-3	26,1	12	46	
	C-4	30,3	14	46	
	C-5	40,1	18	46	
Cellulose D	D-1	15,0	8	50	55
	D-2	19,6	11	54	
	D-3	23,2	13	55	
	D-4	30,3	17	55	
	D-5	40,3	22	55	
Cellulose E	E-1	10,2	6	56	62
	E-2	14,5	9	60	
	E-3	20,4	13	62	
	E-4	25,3	16	62	
	E-5	30,1	19	62	

using the following Eq. (1):

$$(\text{CrI}) (\%) = \frac{(I_{002} - I_{\text{am}})}{I_{002}} \times 100 \quad (1)$$

where  $I_{002}$  is the maximum diffracted intensity by the (002) plane at a  $2\theta$  angle of around  $22^\circ$ , while  $I_{\text{am}}$  is the minimum diffracted intensity at a  $2\theta$  angle of around  $18^\circ$ , representing the intensity scattered by the amorphous region of the sample.

### 2.3. Isotopic exchanges

The ( $\alpha_{\text{iso}}$ ) parameter describes the isotopic exchangeable hydrogen pool versus total hydrogen atoms in a specific matrix and is typically determined by a gas-solid isotopic exchange procedure. The gas-solid isotopic exchange process has already been developed and described in previous publications (Nivesse et al., 2021b; Péron et al., 2018); it is based on a sample set-up vapor phase experiment performed in a confined glove box (Plas-Labs 890-THC) with controlled and stable temperature ( $20.0 \pm 0.1^\circ\text{C}$ ) and relative humidity ( $85\% < \text{RH} < 88\%$ ) parameters. An isotopic steady state with a defined (T/H) ratio is established between a bath of KCl-saturated solution ( $(\frac{T}{H})_{l,\text{bath}}$ ) with controlled tritium activities, a vapor phase confined in a glove box ( $(\frac{T}{H})_{g,\text{vapor}}$ ), the water condensed at the sample surface ( $(\frac{T}{H})_{l,\text{cond}}$ ) and the exchangeable organically bound tritium of the sample ( $(\frac{T}{H})_{s,E-OBT}$ ), which can be described by Eq. (2):

$$\left(\frac{T}{H}\right)_{l,\text{bath}} = \left(\frac{T}{H}\right)_{g,\text{vapor}} = \left(\frac{T}{H}\right)_{l,\text{cond}} = \left(\frac{T}{H}\right)_{s,E-OBT} \quad (2)$$

Isotopic exchanges were conducted on native celluloses following four tritium-enrichment experiments with tritium-rich baths (HTO = 120, 300, 500 and 700 Bq·L<sup>-1</sup>). After 2 days of solid-gas contact

time, the steady state was assumed to be reached, and solid samples were recovered at days 2, 3 and 4 to ensure the reproducibility and steady state of the system. Three baths aliquots were also collected at the steady state and kept at a temperature below 5 °C prior to distillation. After liquid nitrogen immersion and freeze-drying, the solid samples were heat-treated in a tubular furnace (Eraly, France), where the organic matter was transformed into carbon dioxide and combustion water. Liquid samples (combustion waters and baths aliquots) were purified by distillation under atmospheric pressure after pH adjustment with sodium peroxide (Na<sub>2</sub>O<sub>2</sub>) as needed. The tritium activities were measured by means of liquid scintillation counting (PerkinElmer Wallac Quantulus 1220 model) using an Ultima Gold LLT cocktail. The detection limit was estimated at below 1 Bq·L<sup>-1</sup> for a counting time of 24 h and a blank value of 0.7 counts per minute. A quench correction was applied for each measurement according to a quenching curve calculated after calibration with laboratory-prepared quenched standards.

At each steady state, a mean value of the combustion water from each matrix sample  $\left(\frac{T}{H}\right)_{s,OBT}$  was obtained by averaging the measured sample values forming the plateau. A mean value of each saline solution  $\left(\frac{T}{H}\right)_{l,bath}$  was also obtained by averaging the three measured bath aliquot values. The ( $\alpha_{iso}$ ) parameter could thus be determined as the slope of the plot of  $\left(\frac{T}{H}\right)_{s,OBT}$  versus  $\left(\frac{T}{H}\right)_{l,bath}$ , in accordance with the description provided in (Eq. 3):

$$\alpha_{iso} = \frac{\Delta\left(\frac{T}{H}\right)_{s,OBT}}{\Delta\left(\frac{T}{H}\right)_{l,bath}} \quad (3)$$

### 3. Results and discussion

#### 3.1. Crystallinity index (CrI) determination

The XRD patterns for the series of native celluloses are shown in Fig. 1. All celluloses in the series exhibited crystalline peaks attributed to the typical structure of cellulose I at: 2 $\theta$  = 16.1° (110), 22° (200) and 34.7° (004) (Johar et al., 2012; Melikoğlu et al., 2019). Cellulose I is one of the four allomorphic forms of crystalline cellulose (I to IV) and the most common form in a natural source (Chen et al., 2011; Lu et al., 2013). CrI values for celluloses A, B, C, D and E were calculated at 13%,

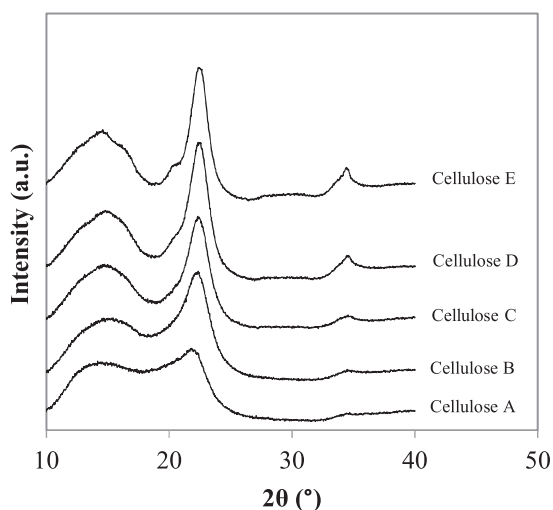


Fig. 1. XRD patterns for the series of five native celluloses from cellulose A through cellulose E.

34%, 46%, 55% and 62%, respectively. From celluloses E and C, the crystallinity ratio decreases as expected due to the partial destruction of crystalline regions during the ball-milling process (Sun and Cheng, 2002).

In order to assess the potential impact of the vapor phase contact during the gas-solid isotopic exchange procedure onto the crystalline structure of the series of native celluloses, X-ray diffraction analysis were conducted before and after the isotopic exchange step. Modifications on both the intensity data of the XRD peaks (for the CrI calculation) and the allomorphic attribution (cellulose I allomorphic form) were thus established to be negligible as no significant change was observed on any of the samples.

#### 3.2. Linear experimental model for the cellulose accessibility determination

Isotopic exchanges were conducted on native celluloses to assess their exchangeable parameter ( $\alpha_{iso}$ ). Accurate values of ( $\alpha_{iso}$ ) equal to 23.8 ± 1.2% (R<sup>2</sup> = 0.999), 19.8 ± 1.6% (R<sup>2</sup> = 0.997), 17.4 ± 2.1% (R<sup>2</sup> = 0.993), 14.4 ± 0.7% (R<sup>2</sup> = 0.999) and 13 ± 1% (R<sup>2</sup> = 0.990) were obtained for celluloses A through E, respectively (Fig. 2). The results on cellulose E exchangeable parameter ( $\alpha_{iso}$ ) were previously presented in Péron et al. (2018).

From these findings, an experimental model based on ( $\alpha_{iso}$ ) vs. CrI was obtained for the series of native celluloses (Fig. 2). A decrease in the exchangeable parameter ( $\alpha_{iso}$ ) can be observed as the degree of crystallinity in the cellulose molecule increases. The crystalline structure of cellulose is represented by an orderly arrangement of D-glucose chains generated by hydrogen bonds. The (1→4)-beta-D-glycosidic bonds and monomer arrangements oriented at 180° are thus responsible for a three-dimensional network (see SI-1). Hence, hydroxyl groups of D-glucose units behave like hydrogen-bound donors at both the intra-molecular and intra-strand levels to provide a stabilized structure to cellulose (Jarvis, 2003; Nishiyama et al., 2003, 2002). As such, a larger proportion of the hydrogen atoms is made inaccessible for isotopic exchange and behaves as non-exchangeable hydrogen, while the degree of crystallinity in the cellulose is increasing.

The experimental model constructed with the series of native celluloses exhibits a linear tendency, with a correlation coefficient equal to 0.9888. Hence, the suggestion of a proportionality ratio is entirely noticeable between the decreases in hydrogen atom accessibility and the extent of the crystalline phase in native cellulose. This dependency can therefore be described as linear (Eq. 4):

$$(\alpha_{iso,celluloses}) = -0.2224 \times (CrI) + 27.01 \quad (4)$$

where ( $\alpha_{iso,celluloses}$ ) is the exchangeable hydrogen atom ratio of the native celluloses series, in %, and (CrI) the crystallinity index from 13% to 62%.

Eq. (4) can thus serve to deduce the ratio of exchangeable hydrogen atoms in native cellulose molecules merely from information on the degree of crystallinity. Hence, these findings could give access to the tritium under the form of NE-OBT storage capacities of native cellulose molecules from a single XRD analysis.

#### 3.3. Environmental matrices applications and limits

Investigations on organically bound tritium distribution and speciation towards cellulose pertain to environmental cellulosic organic matter (Nivesse et al., 2021a; Péron et al., 2018). Consequently, the linear model method established to determine cellulose accessibility requires applicability to cellulosic materials from direct environmental matrices CrI measurements. In environmental matrices, native cellulose may display a wide range of crystallinity rates and is always found in combination with other amorphous to semi-amorphous compounds. An XRD analysis on the entire environmental sample might therefore detect

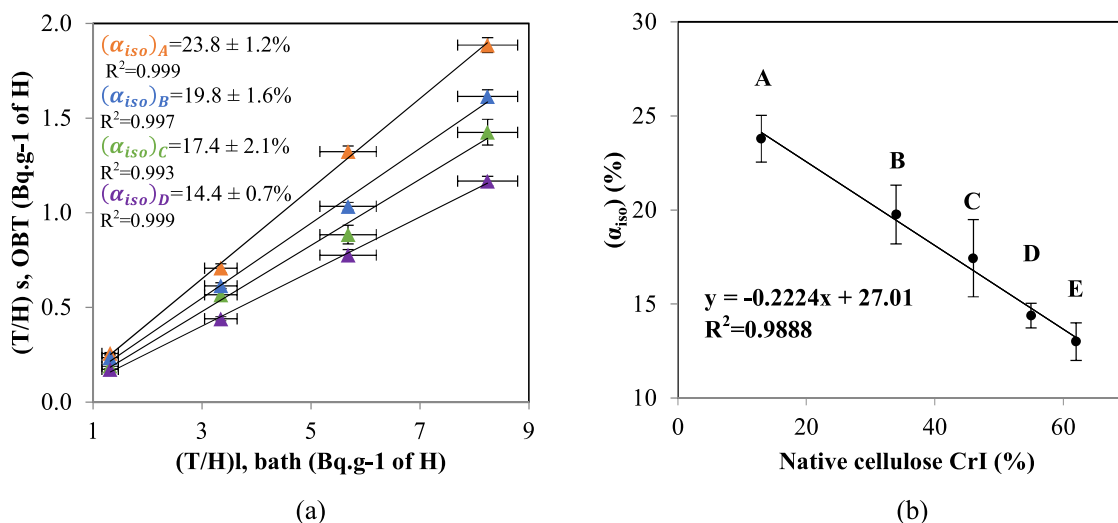


**Fig. 2.** (a) (T/H) of celluloses A through D in the steady state after freeze-drying vs. measured set (T/H) of saline solutions and their associated exchangeable parameter  $(\alpha_{iso})$ . (b) Exchangeable parameter  $(\alpha_{iso})$  vs. crystallinity index (CrI) for the series of five native celluloses from A through E.

the attributed peak at  $22^\circ$  for the cellulose needed for a CrI calculation, yet with a significant impact lowering its intensity in proportion with the amorphous compound content. At some point, the presence of this amorphous phase, provided by the other constituents, may become too great compared to the crystalline phase of the cellulose, making the cellulose peak at  $22^\circ$  undetectable by means of XRD analysis. Nevertheless, it is important to recall here that the main point of this study was to provide reliable information on the accessibility of cellulose OH group from a very simplified and unique sample characterization, as XRD measurements. In order to assess the applicability of the linear experimental model to cellulosic materials from direct measurements in environmental matrices, a study of the significant limits of the CrI parameter determination from XRD analysis was thus carried out. For this purpose, each native cellulose of the series was mixed in different ratios with  $\text{SiO}_2$  amorphous compounds to simulate other non-crystalline fractions of environmental matrices and then analyzed by XRD. CrI (%) values for the modified sequences of increasing cellulose content samples are presented in Table 1. From these results and the cellulose content (in % by weight) of each sample, theoretical CrI values could be calculated and attributed to each of the studied native celluloses (calculated native cellulose CrI (%)) and compared to their actual CrI values (actual native cellulose CrI (%)) (Table 1). For each modified sequence, the cellulose contents were adapted in each sample to achieve the minimum content of cellulose needed to reach the actual calculated CrI value.

Results obtained on the minimum content in % by weight of native celluloses A through E needed to effectively reach an XRD analysis peak at  $22^\circ$  for the correct calculation of their respective CrI values are presented in Fig. 3. For medium to highly crystalline cellulose (i.e. celluloses B through E), the minimum cellulose content needed in samples was found to lie around 20–35% by weight. These values are by far lower than the minimum content of cellulose in natural cellulosic sources like trees or cotton, yet which does approximately correspond to that found in green cellulosic plants like grass or tree leaves (Sun and Cheng, 2002). For very weak crystalline cellulose (cellulose A), only a very high cellulose content was found to be acceptable for an accurate cellulose CrI determination from XRD analysis.

For each of the native cellulose results, it was then estimated that the minimum CrI value calculated from XRD analysis was acceptable as of 12% in an environmental sample to produce an accurate cellulose CrI deduction. Nevertheless, this value remains dependent on the typical internal parameters used in a cellulose analysis of the XRD equipment and could thus be further improved, as needed. Similarly, this

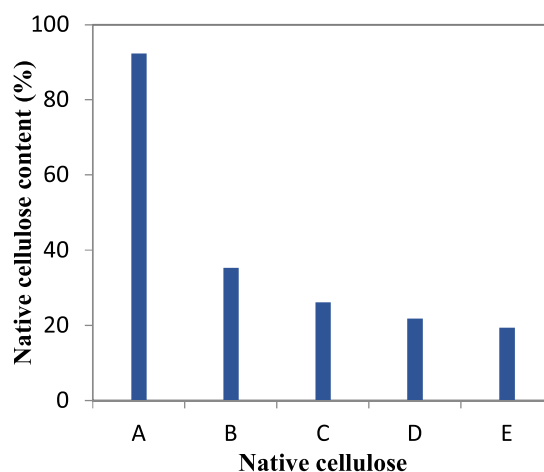


**Fig. 3.** Minimum content (% by weight) of native celluloses A through E needed to effectively reach an XRD analysis peak at  $22^\circ$  for the accurate calculation of their respective CrI (%).

information proves to be relevant when cellulose is the only constituent of the studied matrix whose crystallinity is directly related to the XRD analysis peak at  $22^\circ$ . The linear model is therefore applicable to environmental matrices for cellulose accessibility determination under this condition whenever the CrI value obtained from the matrix sample XRD analysis exceeds 12%. A complementary analysis of the sample composition in cellulose is then needed to deduce the CrI and, hence, the accessibility of the studied cellulose to the main radionuclide released by nuclear power plants, tritium. A fast and efficient analytical process is therefore available for further investigations on organic tritium retention capacities of cellulosic environmental matrices and should also be of great interest to understanding tritium behavior into other major constituents in food chain samples like proteins.

Besides radioactive pollution concerns, the exchange capacities of OH group hydrogen atoms in native cellulose are also important in other hydrogen isotope-related topics, such as investigations on cellulosic material origins within protium and deuterium ratios, to the same extent as in the field of nuclear forensics and retrospective studies on tritium releases into the environment. Most of the functional properties of the cellulose polymer derives from its hydroxyl groups since its chemical reactivity is mainly a function of the high donor reactivity of its OH

groups (Klemm et al., 2005; O'Connell et al., 2008). The hydrogen exchange properties of these OH groups are then heavily involved in the binding processes of metal ions into cellulose fibers, from sorption supported by a hydrated shell exchange with OH groups or electrostatic interactions with carboxyl groups (Kongdee and Bechtold, 2009; Öztürk et al., 2009). As such, the established linear model could also find an interest to estimate the complexing capacities of cellulose with transition metals and actinides in its natural state in environmental samples.

#### 4. Conclusion

To improve the scientific knowledge on tritium behavior prediction in the environment, hydroxyl reactivity has been investigated in a series of native celluloses with an increasing degree of crystallinity using a robust and reliable T/H gas-solid isotopic exchange procedure. A linear relationship was derived between OH group accessibility to tritium and the crystallinity index (CrI) of native celluloses. Since the purpose of this study relies on natural cellulose sources, the applicability of the linear model from direct measurements on environmental matrices was investigated with samples of increasing cellulose content at various crystallinity rates. An acceptable minimum value of 12% for the CrI parameter on environmental matrices could thus be established for the direct deduction of an accurate cellulose content CrI and OH accessibility. These findings then make it possible to determine efficiently, by means of a single and fast XRD analysis, the accessibility of the entire cellulose hydroxyl group pool to tritium bound into environmental matrices. This information can subsequently be used not only to highlight the hydrogen isotopes including tritium storage capacities in cellulosic environmental matrices, but also to evaluate the contribution of other complex compounds involved with structures difficult to characterize, like proteins. Applications to investigations on cellulosic material origins could emerge, to the same extent as retrospective studies of tritium releases and nuclear forensics. In a more fundamental manner, this method of determining hydroxyl group accessibility on native cellulose also provides much relevance in understanding the involvement of the polymer in environmental matrices accessibility to deuterium and tritium, as well as in grasping complexing capacities with metals in the environment.

#### CRedit authorship contribution statement

**A.-L. Nivesse:** Investigation, Validation, Writing – original draft, Writing – review & editing, Visualization. **N. Baglan:** Conceptualization, Methodology, Resources, Writing – review & editing, Supervision. **G. Montavon:** Writing – review & editing, Supervision. **O. Péron:** Conceptualization, Methodology, Resources, Writing – review & editing, Supervision.

#### Declaration of Competing Interest

The authors declare that they have no known competing financial interests or personal relationships that could have appeared to influence the work reported in this paper.

#### Acknowledgements

This work was financed by the CEA Research Center, Subatech Laboratory, France's Loire Valley Regional Council (under the POLLU-SOLS OSUNA Project) and the EDF utility company.

#### Appendix A. Supporting information

Supplementary data associated with this article can be found in the online version at [doi:10.1016/j.jhazmat.2021.126619](https://doi.org/10.1016/j.jhazmat.2021.126619).

#### References

- ASN, 2010. Le Livre Blanc du Tritium, Groupes de Réflexion Menés de Mai 2008 à Avril 2010 Sous L'égide de L'ASN.
- Baglan, N., Cossou, C., Roche, E., Kim, S.B., Croudace, I., Warwick, P., 2018. Feedback of the third interlaboratory exercise organised on wheat in the framework of the OBT working group. *J. Environ. Radioact.* 181, 52–61.
- Chen, W., Yu, H., Liu, Y., Chen, P., Zhang, M., Hai, Y., 2011. Individualization of cellulose nanofibers from wood using high-intensity ultrasonication combined with chemical pretreatments. *Carbohydr. Polym.* 83 (4), 1804–1811.
- Diabaté, S., Strack, S., 1993. Organically bound tritium. *Health Phys.* 65 (6), 698–712.
- Hashem, M.A., Elnagar, M.M., Kenawy, I.M., Ismail, M.A., 2020. Synthesis and application of hydrazono-imidazoline modified cellulose for selective separation of precious metals from geological samples. *Carbohydr. Polym.* Vol. 237, 116177.
- IRSN, 2017. Rapport Actualisation des connaissances Tritium Environnement. (Ed.), Institut de Radioprotection et de Sécurité Nucléaire (IRSN).
- Jarvis, M., 2003. Chemistry: cellulose stacks up. *Nature* 426, 611–612.
- Johar, N., Ahmad, I., Dufresne, A., 2012. Extraction, preparation and characterization of cellulose fibres and nanocrystals from rice husk. *Ind. Crops Prod.* 37 (1), 93–99.
- Kim, S.B., Baglan, N., Davis, P.A., 2013. Current understanding of organically bound tritium (OBT) in the environment. *J. Environ. Radioact.* 126 (1), 83–91.
- Klemm, D., Heublein, B., Fink, H.-P., Bohn, A., 2005. Cellulose: fascinating biopolymer and sustainable raw material. *Angew. Chem. Int. Ed.* 44 (22), 3358–3393.
- Kongdee, A., Bechtold, T., 2009. Influence of ligand type and solution pH on heavy metal ion complexation in cellulosic fibre: model calculations and experimental results. *Cellulose* 16 (1), 53–63.
- Lindh, E.L., Salmén, L., 2017. Surface accessibility of cellulose fibrils studied by hydrogen–deuterium exchange with water. *Cellulose* 24 (1), 21–33.
- Lu, H., Gui, Y., Zheng, L., Liu, X., 2013. Morphological, crystalline, thermal and physicochemical properties of cellulose nanocrystals obtained from sweet potato residue. *Food Res. Int.* Vol. 0 (1), 121–128.
- Luzi, F., Puglia, D., Sarasini, F., Tirillo, J., Maffei, G., Zuorro, A., Lavecchia, R., Kenny, J.M., Torre, L., 2019. Valorization and extraction of cellulose nanocrystals from North African grass: *Ampelodesmos mauritanicus* manuscript. *Carbohydr. Polym.* 209, 328–337.
- Madvoli, E., Kareru, P., Gachanja, A., Mugo, S., Murigi, M., Kairigo, P., Kipyegon, C., Mutembei, J., Njonge, F., 2016. Adsorption of selected heavy metals on modified nano cellulose. *Int. Res. J. Pure Appl. Chem.* 12, 1–9.
- Melikoglu, A.Y., Bilek, S.E., Cesur, S., 2019. Optimum alkaline treatment parameters for the extraction of cellulose and production of cellulose nanocrystals from apple pomace. *Carbohydr. Polym.* 215 (1), 330–337.
- Nishiyama, Y., Langan, P., Chanzy, H., 2002. Crystal structure and hydrogen-bonding system in cellulose II-beta from synchrotron X-ray and neutron fiber diffraction. *J. Am. Chem. Soc.* 124, 9074–9082.
- Nishiyama, Y., Sugiyama, J., Chanzy, H., Langan, P., 2003. Crystal structure and hydrogen bonding system in cellulose II-alpha from synchrotron X-ray and neutron fiber diffraction. *Am. Chem. Soc.* 125, 14300–14306.
- Nivesse, A.-L., Baglan, N., Montavon, G., Granger, G., Péron, O., 2021a. Cellulose, proteins, starch and simple carbohydrates molecules control the hydrogen exchange capacity of bio-indicators and foodstuffs. *Chemosphere*.
- Nivesse, A.-L., Baglan, N., Montavon, G., Granger, G., Péron, O., 2021b. Non-intrusive and reliable speciation of organically bound tritium in environmental matrices. *Talanta*.
- Nivesse, A.-L., Thibault de Chanvalon, A., Baglan, N., Montavon, G., Granger, G., Péron, O., 2020. An overlooked pool of hydrogen stored in humic matter revealed by isotopic exchange: implication for radioactive 3H contamination. *Environ. Chem. Lett.* 18 (2), 475–481.
- Öztürk, H.B., Vu-Manh, H., Bechtold, T., 2009. Interaction of cellulose with alkali metal ions and complexed heavy metals. *Lenzinger Berichte*, 142–150.
- O'Connell, D.W., Birkinshaw, C., O'Dwyer, T.F., 2008. Heavy metal adsorbents prepared from the modification of cellulose: a review. *Bioresour. Technol.* 99 (15), 6709–6724.
- Péron, O., Fourré, E., Pastor, L., Gégout, C., Reeves, B., Lethi, H.H., Rousseau, G., Baglan, N., Landesman, C., Siclet, F., Montavon, G., 2018. Towards speciation of organically bound tritium and deuterium: Quantification of non-exchangeable forms in carbohydrate molecules. *Chemosphere* 196 (1), 120–128.
- Péron, O., Gégout, C., Reeves, B., Rousseau, G., Montavon, G., Landesman, C., 2016. Anthropogenic tritium in the Loire River estuary, France. *J. Sea Res.* 118, 69–76.
- Reishofer, D., Spirk, S., 2015. Deuterium and Cellulose: A Comprehensive Review. *Cellulose Chemistry and Properties: Fibers, Nanocelluloses and Advanced Materials*, 271, 93–114.
- Segal, L., Creely, J.J., Martin, A.E., Conrad, C.M., 1959. An empirical method for estimating the degree of crystallinity of native cellulose using the X-ray diffractometer. *Text. Res. J.* 29 (10), 786–794.
- Sepall, O., Mason, S.G., 1961. Hydrogen exchange between cellulose and water: II. Interconversion of accessible and inaccessible regions. *Can. J. Chem.* 39 (10), 1944–1955.
- Song, J., Xiong, Y., Lang, L., Shi, Y., Ba, J., Jing, W., He, M., 2019. Radiochemical reaction of DT/T2 and CO under high pressure. *J. Hazard. Mater.* 378, 120720.
- Sun, Y., Cheng, J., 2002. Hydrolysis of lignocellulosic materials for ethanol production: a review. *Bioresour. Technol.* 83, 1–11.
- Trache, D., Hussin, M.H., Hui Chuin, C.T., Sabar, S., Fazita, M.R.N., Taiwo, O.F.A., Hassan, T.M., Haafiz, M.K.M., 2016. Microcrystalline cellulose: isolation, characterization and bio-composites application—a review. *Int. J. Biol. Macromol.* 93 (1), 789–804.